

Esculetin, a coumarin derivative, exerts *in vitro* and *in vivo* antiproliferative activity against hepatocellular carcinoma by initiating a mitochondrial-dependent apoptosis pathway

J. Wang^{1,2}, M.L. Lu², H.L. Dai², S.P. Zhang², H.X. Wang² and N. Wei¹

¹The First Affiliated Hospital, Liaoning Medical University, Jinzhou, China

²Key Laboratory of Cardiovascular and Cerebrovascular Drug Research, Liaoning Province, Liaoning Medical University, Jinzhou, China

Abstract

This study investigated the *in vitro* and *in vivo* antiproliferative activity of esculetin against hepatocellular carcinoma, and clarified its potential molecular mechanisms. Cell viability was determined by the MTT (tetrazolium) colorimetric assay. *In vivo* antitumor activity of esculetin was evaluated in a hepatocellular carcinoma mouse model. Seventy-five C57BL/6J mice were implanted with Hepa1-6 cells and randomized into five groups (n = 15 each) given daily intraperitoneal injections of vehicle (physiological saline), esculetin (200, 400, or 700 mg·kg⁻¹·day⁻¹), or 5-Fu (200 mg·kg⁻¹·day⁻¹) for 15 days. Esculetin significantly decreased tumor growth in mice bearing Hepa1-6 cells. Tumor weight was decreased by 20.33, 40.37, and 55.42% with increasing doses of esculetin. Esculetin significantly inhibited proliferation of HCC cells in a concentration- and time-dependent manner and with an IC₅₀ value of 2.24 mM. It blocked the cell cycle at S phase and induced apoptosis in SMMC-7721 cells with significant elevation of caspase-3 and caspase-9 activity, but did not affect caspase-8 activity. Moreover, esculetin treatment resulted in the collapse of mitochondrial membrane potential *in vitro* and *in vivo* accompanied by increased Bax expression and decreased Bcl-2 expression at both transcriptional and translational levels. Thus, esculetin exerted *in vitro* and *in vivo* antiproliferative activity in hepatocellular carcinoma, and its mechanisms involved initiation of a mitochondrial-mediated, caspase-dependent apoptosis pathway.

Key words: Esculetin; Apoptosis; Hepatocellular carcinoma; Mitochondrial-dependent pathway; Antitumor activity

Introduction

Hepatocellular carcinoma (HCC) is the fifth most common cancer and the second leading cause of cancer-related deaths worldwide (1). The evidence suggests that the incidence of HCC is rising, making it a major health problem, especially in China, where the incidence of HCC has increased by 50% over the past 10 years (2). The current treatments for HCC are surgery and chemotherapy. However, most HCC patients are not candidates for surgical resection because, at the time of diagnosis, the tumor may be too large or has expanded into nearby major blood vessels or metastasized (3). In addition, the efficacy of chemotherapy is not high, and the side effects are often difficult to tolerate. Thus, novel anticancer therapeutic agents for treatment of HCC are urgently needed.

Natural products have been a primary source of discovery and development of anticancer drugs and novel natural products that have antitumor activity against HCC may be found. Esculetin, a phenolic compound that occurs in various plants, has displayed beneficial pharmacological and biochemical properties including anticancer, anti-inflammatory, neuroprotective, and antioxidant activity (4-8). Esculetin was shown to have anticancer activity in human colon cancer, breast cancer, human leukemia, and cervical cancer, and to inhibit cell proliferation in human colon cancer through the Ras/ERK1/2 pathway (9). Park et al. (10) reported that esculetin suppressed the c-Jun N-terminal kinase (JNK) and extracellular-signal-regulated kinase (ERK) pathways, and induced apoptosis in human

Correspondence: Hongxin Wang: <hongxinwang@lnmu.edu.cn>; Ning Wei: <chinaweining@yahoo.com>

Received April 26, 2014. Accepted October 8, 2014. First published online December 12, 2014.

leukemia U937 cells. In addition, esculletin was shown to sensitize HepG2 cells to the effects of taxol (11). However, *in vitro* and *in vivo* studies have not yet confirmed the therapeutic effect of esculletin on growth of HCC or revealed its molecular mechanisms of action.

This study evaluated the *in vivo* and *in vitro* antitumor effect of total alkaloids of esculletin in a mouse xenograft model and in cultures of SMMC-7721 hepatocellular carcinoma cells. The potential mechanism of esculletin against HCC is also described.

Material and Methods

Reagents

The isolation, identification, and purity assessment of esculletin were performed in our laboratory as previously described (12). 5-Fu was obtained from Tianjing Jinyao Anjisuan Medicine Co., Ltd. (China). The Annexin V-FITC apoptosis detection kit was purchased from Beijing Biosea Biotechnology Co., Ltd. (China). Propidium iodide (PI), dimethyl sulfoxide (DMSO), and 3-(4,5-dimethylthiazol)-2,5-diphenyltetrazolium bromide (MTT) were obtained from Amresco (USA). β -actin, caspase-3/-9, Bcl-2 and Bax antibodies were from Beijing Biosynthesis Biotechnology (China). 5,5',6,6'-tetrachloro-1,1',3,3'-tetraethyl-benzimidazol-carbocyanine iodide (JC-1) and the RT-PCR kit were obtained from Beyotime Institute of Biotechnology (China). Dulbecco's modified Eagle's medium (DMEM) was from Gibco (USA) and trypsin from Hyclone (USA).

Animals

The experimental protocols were approved by the ethics committee of Liaoning Medical College for the use of experimental animals for research and teaching. Seventy-five 6-week-old C57BL/6J male mice (20-22 g) were purchased from the Animal Centre of Chinese Medical University. All mice were housed in a specific-pathogen free laboratory. The mice were fed standard rodent pellets and allowed free access to filtered water. All experimental procedures were performed in accordance with the Guidelines of Animal Experiments from the Committee of Medical Ethics, National Health Department of China.

Animal tumor model

The Hepa1-6 cell line was purchased from the Type Culture Collection of the Chinese Academy of Sciences, Shanghai, China. Cells were cultured in DMEM medium with 10% fetal calf serum (FCS) and 90% DMEM and maintained in a humidified atmosphere of 5% CO₂ at 37°C. Hepa1-6 cells were inoculated subcutaneously in the right axilla of C57BL/6J mice (1×10^7 viable cells/mL) to establish a xenograft model. Three days after implantation, mice were randomized into 5 groups ($n = 15$ each) and injected intraperitoneally with vehicle (physiological saline), esculletin (200, 400, or 700 mg·kg⁻¹·day⁻¹), or 5-Fu (200 mg·kg⁻¹·day⁻¹) as a positive control for 15 days. *In vivo* antitumor activity

of esculletin was evaluated by weight and inhibition rate. Tumor inhibition (%) was measured by the following ratio: $(1 - W_{\text{Treated}}) / W_{\text{Control}} \times 100\%$. W_{Treated} and W_{Control} were the average tumor weights in treated and control mice.

Cell culture and viability assay

The SMMC-7721 human hepatocellular carcinoma cell line was obtained from the Scientific Experiment Center of Liaoning Medical College (China) and maintained at 37°C in humidified 95% air and 5% CO₂ in DMEM supplemented with 10% heat-inactivated fetal bovine serum (FBS). The cells were subcultured at 80% confluency.

Cell proliferation was assayed as previously described (13). SMMC-7721 cells were resuspended in DMEM with 10% FBS and seeded onto 96-well plates at a density of 1×10^4 cells/mL in 0.1 mL medium and cultured for 24 h. The cells were treated with various concentrations of esculletin for 24, 48, and 72 h. At the end of the treatment, 20 μ L MTT was added to each well, and the cells were incubated for another 4 h. The purple-blue MTT formazan precipitate was dissolved in 150 μ L DMSO and was measured at 570 nm using a multi-mode microplate reader (BioTek Instruments, Inc., USA). All measurements were performed three times. Growth inhibition (%) was measured by the following ratio: $(1 - A_{\text{Treated}} / A_{\text{Control}}) \times 100\%$. A_{Treated} and A_{Control} were the average absorbance of three parallel experiments from treated and control groups. IC₅₀ was the concentration that caused 50% inhibition of cell viability and was calculated by the logit model.

Cell cycle analysis

SMMC-7721 cells (1×10^5 /mL cells per culture flask) were incubated for 24 h, and harvested after esculletin (0, 1.12, 2.24, or 4.48 mM), or 5-FU (0.77 mM) treatment for 48 h. The cells were washed in cold PBS two or three times and fixed in 70% ice-cold ethanol at 4°C overnight. Cells were then stained with 0.5 mg/mL PI containing 0.5 mg/mL RNase and incubated at 4°C for 30 min in the dark. Cell cycle analysis was done by flow cytometry using a FACSCalibur system (Becton Dickinson, USA).

Determination of caspase activity

Caspase-3, -9, and -8 activity induced by esculletin was determined by colorimetric assay kits (Beyotime Institute of Biotechnology) according to the manufacturer's instructions. All measurements were performed 3 times, and caspase activity was determined by measuring changes in absorbance at 405 nm using an ELISA reader (BioTek Instruments, Inc.).

Apoptosis assay

Apoptosis of HCC cells was determined by flow cytometry analysis using an annexin assay. For the *in vivo* assay, tumor tissue was immersed in physiological saline and a cell suspension was prepared in a tissue homogenizer. For the *in vitro* assay, SMMC-7721 cells were

harvested as previously described, concentrated, and washed with cold PBS. Cells were stained with Annexin V-FITC using an assay kit (BD Biosciences, USA) according to the manufacturer's instructions. Data were analyzed using the Bioconsort software (USA).

Mitochondrial membrane potential assessment

Mitochondrial membrane potential (MMP, $\Delta\Psi_m$) was determined by flow cytometric analysis of JC-1 staining. JC-1 is a fluorescent dye that reflects changes in MMP in living cells. Mitochondrial injury results in reduced MMP and leads to an increase in green fluorescence. MMP is reported as the ratio of red to green fluorescence intensity. Cells were obtained as previously described and JC-1 (Beyotime Institute of Biotechnology) staining was performed according to the manufacturer's instructions. Relative fluorescence intensities were monitored by flow cytometry (FACSCalibur). Similarly, 200 g tumor tissue slices obtained from C57BL/6J mice used in the *in vivo* experiments were homogenized with a glass homogenizer (Haimen Hua Kai Experiment Glass Instrument Co., Ltd., China), and the homogenate was centrifuged at 1500 g for 10 min. The supernatant was centrifuged again and resuspended with 50 μ L Store Buffer. Then MMP in tumor tissues was assayed using a biopsy MMP kit (Genmed Scientific, China) and monitored by flow cytometry (FACSCalibur).

Western blot analysis

Cells were prepared as previously described. After 24 h, cells were harvested, washed with PBS, and lysed in lysis buffer. Lysates were centrifuged at 12,500 g for 5 min at 4°C, and the total protein concentration was measured. The protein samples were fractionated using 10% sodium dodecyl sulfate-polyacrylamide gel electrophoresis (SDS-PAGE) and transferred to polyvinylidene difluoride (PVDF) membranes. The membranes were incubated with primary antibodies for 16 h at 4°C, followed by secondary antibodies conjugated to horseradish peroxidase (1:1000) for 1 h at 37°C. β -Actin was used to normalize protein loading.

Tumor tissue was thawed in lysis buffer and homogenized using a dounce homogenizer (Haimen Hua Kai Experiment Glass Instrument Co., Ltd.). The homogenate was then centrifuged at 12,000 g for 30 min at 4°C. The protein concentration of the supernatants was determined by the Bradford method. Each sample was then loaded into alternate lanes for gel electrophoresis. Membrane transfer was performed and incubated with rabbit antibody against Bax and Bcl-2. β -Actin was used as the loading control. Images were captured and analyzed with the Quantity One software (Bio-Rad Laboratories, USA).

RT-PCR analysis

Bax and *Bcl-2* gene expression was detected by RT-PCR. Total RNA was extracted from tumor tissues using Trizol according to the manufacturer's instructions (Promega, USA). cDNA was synthesized using SuperScript III Reverse

Transcriptase (Invitrogen, USA). The sequences of the primers used for amplification of *Bcl-2*, *Bax* and *GAPDH* transcripts were as follows: *Bax* forward, 5'-CCA GGA TGC GTC CAC CAA GAA-3' and reverse, 5'-AGC AAA GTA AAG AGG GCA ACC AC-3'; *Bcl-2* forward, 5'-CTC TGG TTG GGA TTC CTA CGG-3' and reverse, 5'-CGG CAT GAT CTT CTG TCA AGT TTA-3'; *GAPDH* forward, 5'-TG TTC CTA CCC CCA ATG TGT CCG TC-3' and reverse, 5'-CT GGT CCT CAG TGT AGC CCA AGA TG-3'. Initial template denaturation was performed for 5 min at 95°C. The cycle profiles were programmed as follows: 2 s at 95°C (denaturation), 20 s at 60°C (annealing), and 30 s at 72°C (extension). The PCR reaction products were applied to a 2% agarose gel and separated by electrophoresis for

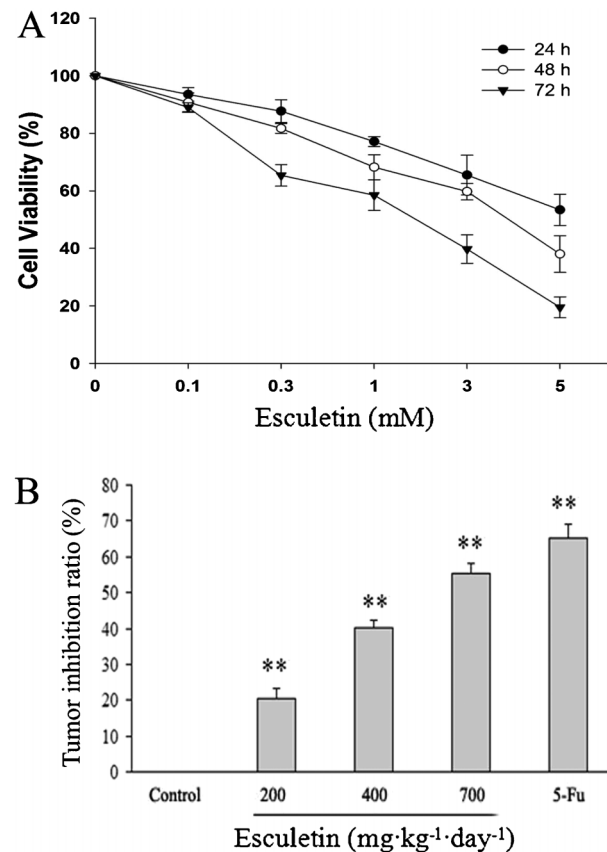


Figure 1. Effect of esculetin on the growth of hepatocellular carcinoma *in vivo* and *in vitro*. SMC7721 cells were seeded onto 96-well plates, and then treated with different concentrations of esculetin for 24, 48, and 72 h. Cell viability was determined by MTT assay (A). Hepa1-6 cells were inoculated subcutaneously at the right axilla of C57BL/6J mice (1×10^7 viable cells/mL) to establish the xenograft model. Tumor inhibition (B) is reported as a ratio: tumor inhibition (%) = $(1 - W_{\text{Treated}}) / W_{\text{Control}} \times 100\%$. W_{Treated} and W_{Control} are the average tumor weights in treated and control mice, respectively. Data are reported as means \pm SD for n = 15. **P < 0.01 vs control group (one-way ANOVA followed by Bonferroni's test).

40 min. The expression intensity of Bax and Bcl-2 mRNA is reported as the ratio of the photodensities of Bax and Bcl-2 to that of GAPDH.

Statistical analysis

Data were analyzed using the SPSS 17.0 software (IBM, USA). Results are reported as means \pm SD for each group and evaluated by one-way ANOVA. $P < 0.05$ was considered to be statistically significant.

Results

Esculetin inhibited growth of hepatocellular carcinoma both *in vivo* and *in vitro*

Cells were exposed to various concentrations of

esculetin for 24, 48, or 72 h and cell proliferation was determined by MTT assay. Esculetin significantly inhibited the viability of hepatocellular carcinoma cells ($P < 0.05$) in a dose- and time-dependent manner (Figure 1A). The IC_{50} values of esculetin against SMMC-7721 cells at 72 h was 2.24 mM. We also evaluated the antitumor effect of esculetin *in vivo* by establishing a xenograft tumor model in C57BL/6J mice by injection of Hepa1-6 cells. As shown in Figure 1B, the tumor inhibition rates of esculetin (200, 400, and 700 $mg \cdot kg^{-1} \cdot day^{-1}$) were 20.33, 40.37, and 55.42%, respectively. Of note, even the highest dose of esculetin had no evident effect on the body weight of xenograft mice. Esculetin did not exhibit toxicity in this animal study. Taken together, our findings suggested that esculetin suppressed the growth of hepatocellular carcinoma both *in vitro* and *in vivo* (Figure 1).

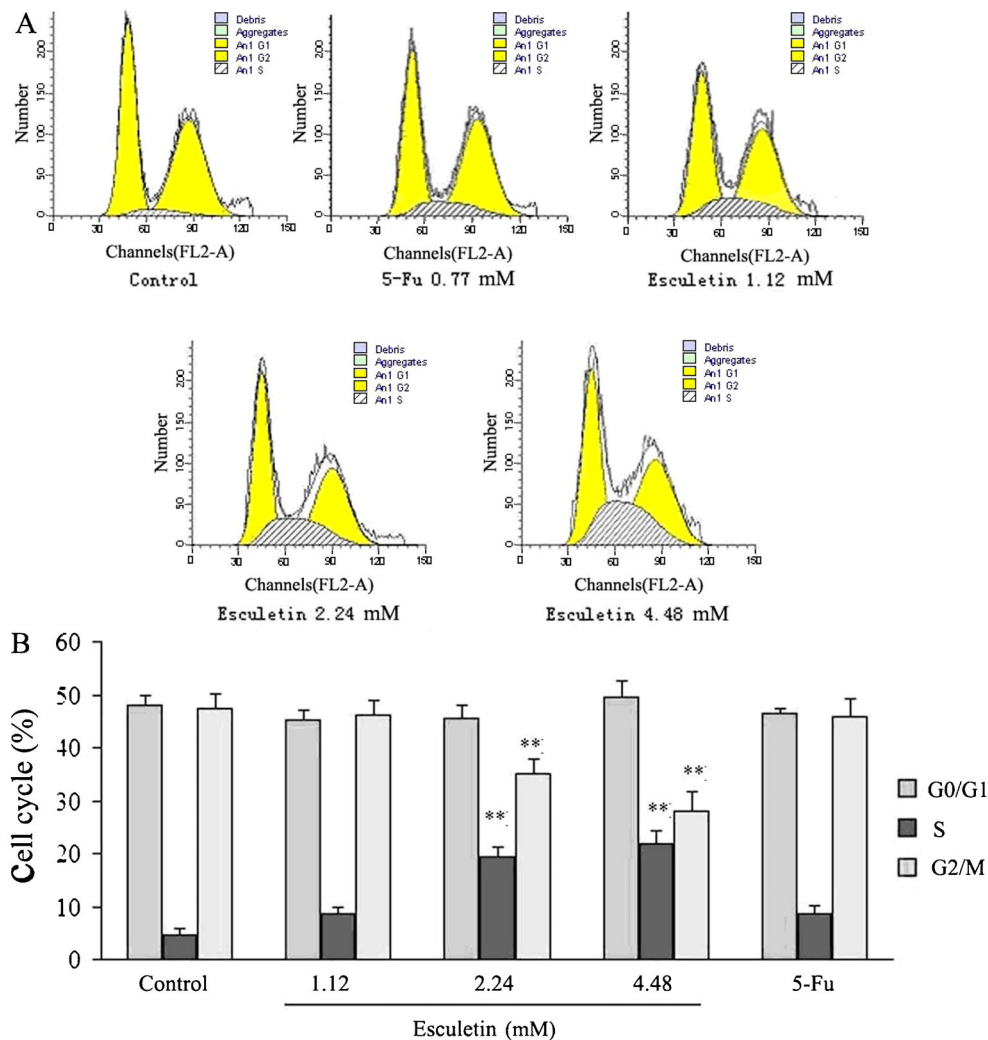


Figure 2. Effects of esculetin on the cell cycle of SMMC-7721. SMMC-7721 cells were seeded at a density of 1×10^5 /mL cells per culture flask for 24 h, and harvested after treatment with esculetin (0, 1.12, 2.24, and 4.48 mM) and 5-FU (0.77 mM) for 48 h. Cell cycle distributions in SMMC-7721 cells were determined by PI staining and flow cytometry analysis. Data were analyzed using the Bioconsort software and are reported as means \pm SD. ** $P < 0.01$ vs control group (one-way ANOVA followed by Bonferroni's test).

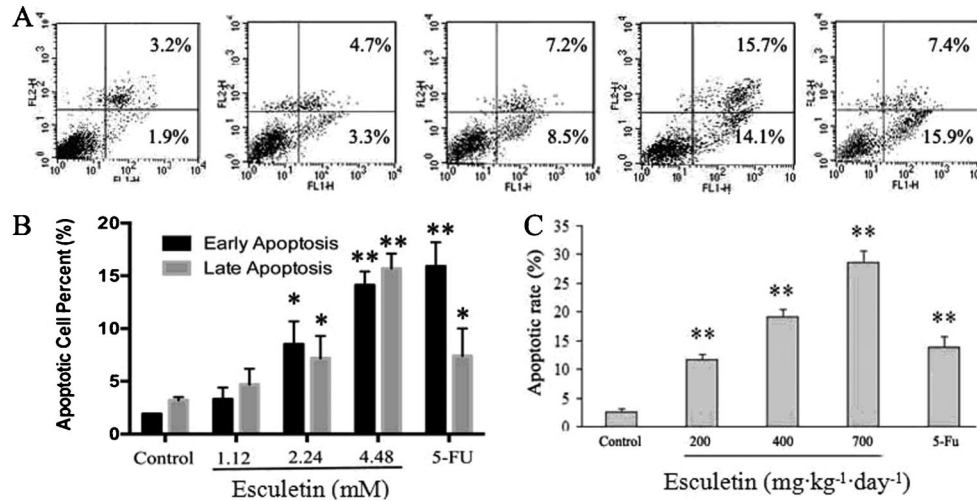


Figure 3. Esculetin induced apoptosis of hepatocellular carcinoma (HCC). SMMC-7721 cells were grouped and harvested after esculetin (0, 1.12, 2.24, and 4.48 mM) and 5-Fu (0.77 mM) treatment for 48 h (A and B). Early and late apoptosis of HCC cells was determined by flow cytometry analysis using a PI-Annexin V-FITC kit. Data were analyzed using Bioconsort software and are reported as means \pm SD. In addition, apoptotic cells (C) in tumors were also detected and analyzed using the Bioconsort software and are reported as means \pm SD for $n = 15$. ** $P < 0.01$ vs control group (one-way ANOVA followed by Bonferroni's test).

Effects of esculetin on the cell cycle distribution in SMMC-7721 cells

The *in vitro* and *in vivo* assays of esculetin antiproliferative activity revealed effects on cell-cycle distribution. SMMC-7721 cells were incubated with esculetin for 48 h and cell cycle distribution was assayed by FACS. As seen in Figure 2, esculetin at 2.24 and 4.48 mM significantly increased the percentage of cells in S phase from 4.7% to 19.5, and 22.2%, respectively ($P < 0.05$). In addition, the percentages of cells in G2/M phase decreased from 47.3% (control) to 35.0 and 28.3%, respectively ($P < 0.01$; Figure 2). These results suggest that esculetin blocked the cell cycle at S phase.

Esculetin induced apoptosis in tumor and SMMC-7721 cells

Apoptosis of cells was analyzed by flow cytometry using PI-Annexin V-FITC. As shown in Figure 3A and B, after treatment with esculetin and 5-Fu, the early and late apoptotic cells increased significantly in a dose-dependent manner. Apoptosis levels were 13.9, 19.1, 28.6, and 14.7% when C57BL/6J mice were treated with low-, medium-, or high-dose (200, 400, or 700 mg·kg⁻¹·day⁻¹) esculetin, and 5-Fu, respectively ($P < 0.05$). Esculetin treatment was thus consistently shown to induce apoptosis both *in vivo* and *in vitro*.

Esculetin led to the loss of MMP *in vivo* and *in vitro*

The effect of esculetin on MMP was examined *in vivo* and *in vitro* by JC-1 staining followed by FACS analysis. Intact mitochondrial membranes allow accumulation of JC-1 in the mitochondria, in which it will generate red

fluorescence. Once loss of MMP occurs, JC-1 cannot accumulate in the mitochondria where it will remain as a monomer in the cytosol and fluoresce green light (14). Therefore, collapse of mitochondrial potential during apoptosis is indicated by an increase in the ratio of green to red fluorescence. When tumor-bearing C57BL/6J mice were treated with esculetin for 15 consecutive days, the MMP of the tumor tissues was significantly decreased compared with that of untreated animals ($P < 0.01$). The green fluorescence ratio in low-, medium-, or high-dose treatment groups was 17.5, 36.7, and 48.5%, respectively, significantly higher than that of the untreated group. Exposure of cells to esculetin (0, 1.12, 2.24, or 4.48 mM) for 48 h led to significant decreases of MMP level. This result suggests that esculetin caused the loss of mitochondrial membrane potential in HCC in a dose-dependent manner (Figure 4).

Esculetin induced activation of caspase-3, -8, and -9 in SMMC-7721 cells

Caspases are known to be a pivotal regulator in the process of cellular apoptosis (15). Thus, we investigated effects of esculetin on the activation of caspase-3, -8, and -9 by a colorimetric assay. We found that esculetin significantly induced activation of caspase-9 and -3 in SMMC-7721 cells ($P < 0.05$ vs untreated cells), but did not affect caspase-8 activity. The results indicated that esculetin treatment induced apoptosis in SMMC-7721 cells through an intrinsic apoptosis pathway (Figure 5).

Effect of esculetin on Bcl-2 and Bax expression

Bcl-2 family proteins play an important role in the

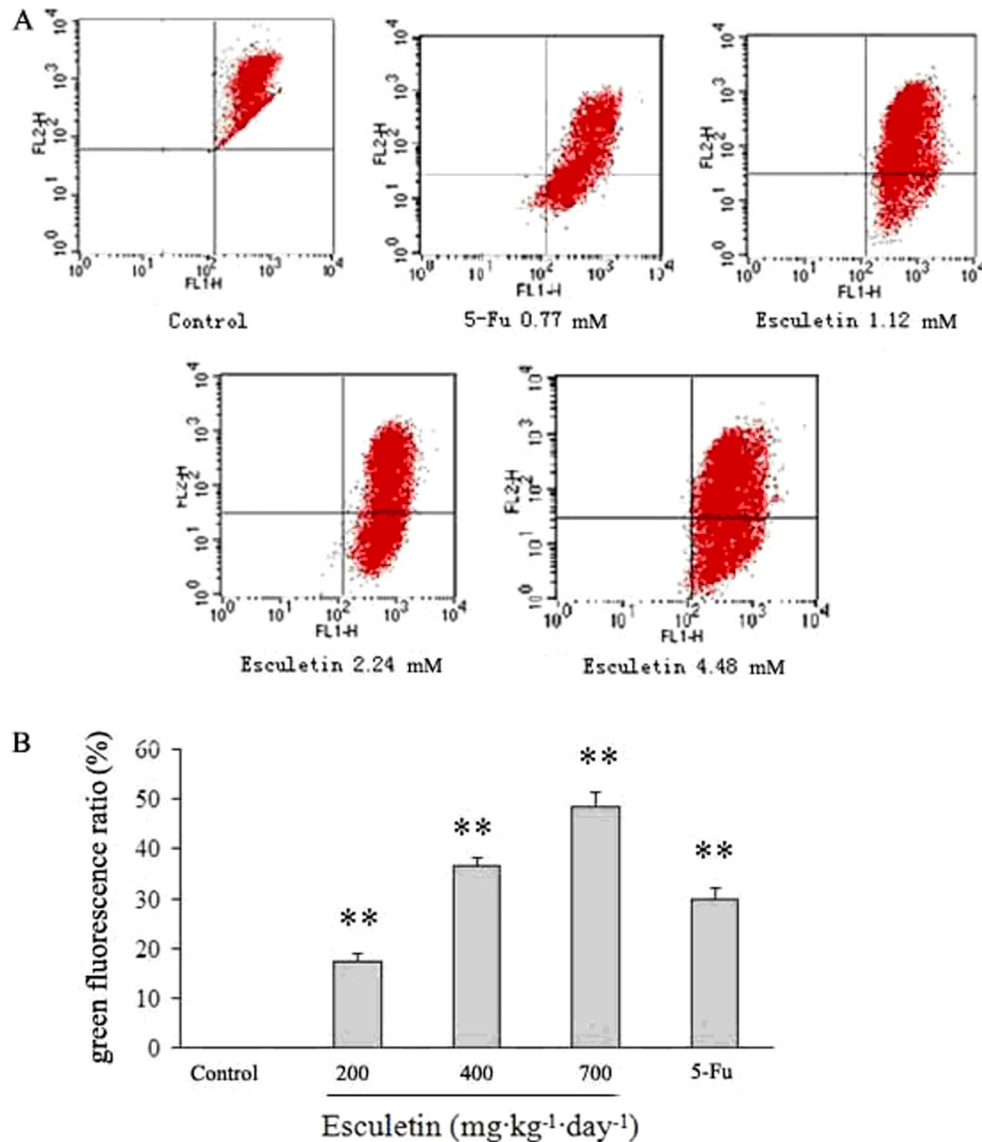


Figure 4. Esculetin caused loss of mitochondrial potential in SMMC-7721 cells (A) and *in vivo* (B). Mitochondrial membrane potential (MMP, $\Delta\Psi\text{m}$) was determined by flow cytometry analysis with JC-1 staining. Data were analyzed using the Bioconsort software and are reported as mean \pm SD for $n = 15$. ** $P < 0.01$ vs control group (one-way ANOVA followed by Bonferroni's test).

mitochondria-mediated apoptosis pathway, including Bax and Bcl-2 (16). To further understand the molecular mechanism of esculetin-mediated cellular apoptosis, expression of Bcl-2 and Bax was evaluated. As shown in Figure 6A and B, expression of Bcl-2 and Bax were significantly changed after esculetin treatment ($P < 0.01$). Esculetin resulted in an increase of Bax (proapoptotic) protein expression in a dose-dependent manner and a decrease of Bcl-2 (antiapoptotic) protein expression in tumors of both C57BL/6J mice and SMMC-7721 cells. These results suggest that esculetin caused an increase of the Bax/Bcl-2 ratio that might be involved in mitochondria-dependent apoptosis.

In addition, expression of Bcl-2 and Bax in C57BL/6J mice was assayed by RT-PCR. As shown in Figure 6C, expression of Bcl-2 and Bax mRNA was consistent with expression of the corresponding proteins. Treatment with esculetin resulted in a significant decrease of antiapoptotic Bcl-2 mRNA levels in Hepa1-6 tumors, whereas that of proapoptotic Bax was significantly increased ($P < 0.05$).

Discussion

Recently, several groups reported that esculetin had antitumor activity in many types of cancer. For instance,

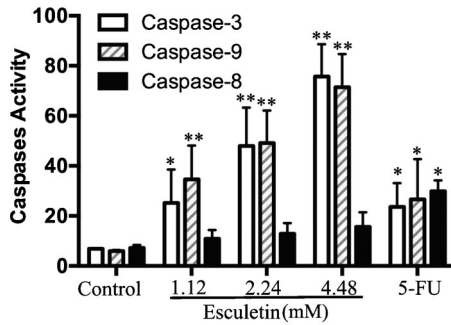


Figure 5. Effect of esculetin on the activity of caspases in SMMC-7721 cells. SMMC-7721 cells were grouped and harvested after esculetin (0, 1.12, 2.24, and 4.48 mM) and 5-FU (0.77 mM) treatment for 48 h. The caspase activities induced by esculetin were determined by colorimetric assays using caspase-3, -9, and -8 activation kits, following the manufacturer's instructions. All measurements were performed 3 times and the activity of caspases was determined by measuring changes in absorbance at 405 nm using the ELISA reader. Data are reported as means \pm SD for 6 in each group. * $P < 0.05$, ** $P < 0.01$ vs control group (one-way ANOVA followed by Bonferroni's test).

esculetin induced apoptosis of human NB4 acute promyelocytic leukemia cells (17) and also initiated apoptosis in U937 human leukemia cells through activation of JNK and ERK (9). Although several *in vitro* studies have demonstrated the inhibition of cancer cell proliferation by esculetin, there are few *in vivo* studies of its therapeutic effect in HCC. This study evaluated the antitumor activity of esculetin by its effects on cell proliferation and tumor growth in a C57BL/6J mouse xenograft model. Our data showed that esculetin significantly inhibited the growth of HCC. Of note, esculetin had no obvious toxicity in this animal study.

Based on the inhibitory effect of esculetin on growth of HCC, the potential mechanism of esculetin action was studied. Apoptosis is a key process mediated by chemotherapeutic agents and it contributes to efficacy (18). Esculetin-induced apoptosis has been reported in other types of cancer including human colon cancer, human oral cancer, and lung cancer (9,19-21). Herein, our results showed that esculetin could effectively induce apoptosis in both tumor-bearing mice and SMMC-7721 cells. The apoptotic rate reached 55.42% after treatment with high-dose esculetin *in vivo*. In addition, we also investigated the effect of esculetin on the cell cycle. Esculetin treatment caused S-phase arrest in SMMC-7721 cells. These results demonstrated that esculetin inhibited tumor cell growth by arresting the cell cycle in S phase and inducing apoptosis.

Apoptosis-signaling cascades can be divided into two major pathways: a death-receptor-induced extrinsic pathway and a mitochondria-apoptosome-mediated intrinsic pathway (22). Apoptosis is modulated by active caspases that are derived from inactive zymogens in a cascade of sequential cleavage reactions (23). Caspase-8 is involved in the death-receptor-induced extrinsic apoptosis pathway

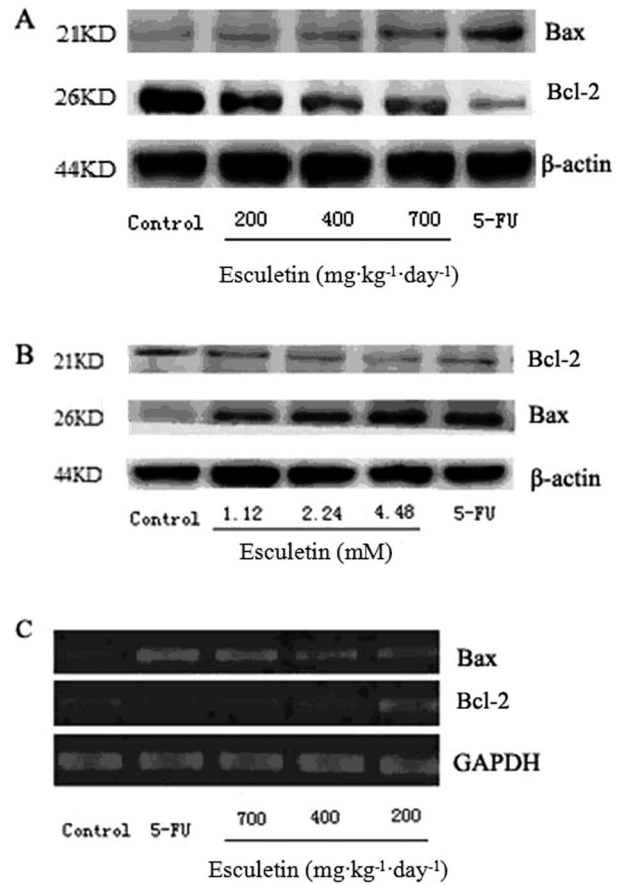


Figure 6. Effect of esculetin on the expression of Bax and Bcl-2. The protein expression of Bcl-2 and Bax was determined by Western blot analysis (A and B). The mRNA expression of Bax and Bcl-2 was detected by RT-PCR (C).

while caspase-9 is associated with the mitochondria apoptotic pathway (24,25). Caspase-9 is the initiator of the mitochondria apoptotic pathway, which is activated in a complex termed the apoptosome by the scaffold protein Apaf-1 and its cofactor cytochrome C. Cytochrome C acts in association with other cytosolic factors to cause activation of executioner caspase-3, in turn leading to downstream apoptotic events (26). In this study, our results demonstrated that esculetin induced apoptosis through the activation and cleavage of caspase-3 and -9.

The Bcl-2 family includes regulators of the mitochondria-mediated apoptosis pathway, such as Bax and Bcl-2 (27). Following an apoptosis signal, the proapoptotic protein Bax translocates to the outer mitochondrial membrane, promoting permeabilization and the release of various apoptotic factors. Antiapoptotic Bcl-2 has been shown to prevent apoptosis by forming a heterodimer with a proapoptotic member, such as Bax, resulting in neutralization of proapoptotic effects. Bcl-2 can also influence the permeability of the intracellular membranes of mitochondria

and the activation of caspase-3 (28). Therefore, the balance of the expression of Bcl-2 and Bax proteins is crucial for cell survival and cell death (29,30). In this investigation, we found that Bax expression was significantly elevated while Bcl-2 expression was significantly decreased both *in vitro* and *in vivo*. Consistent with this, the transcriptional levels of Bax and Bcl-2 mRNA were changed in Hepa1-6 tumors after esculetin treatment, which ultimately resulted in an increase in the Bax/Bcl-2 ratio and activation of the caspase cascade (Figure 6). In addition, our results showed that esculetin treatment induced loss of MMP. Therefore, esculetin induced apoptosis in HCC through the mitochondria-mediated intrinsic pathway. Taken together, our findings suggest that cellular apoptosis mediated in HCC by esculetin *in vivo* and *in vitro* was dependent on caspase-9 and

-3 and Bcl-2 family proteins.

In summary, *in vitro* and *in vivo* antitumor effects in human HCC were associated with S-phase arrest and apoptosis. In addition, esculetin elevated the Bax/Bcl-2 ratio, activated caspase-3 and -9, and induced the mitochondrial-mediated apoptosis pathway in HCC cells. The present study provides evidence supporting esculetin as a potential therapeutic agent for the treatment of hepatocellular carcinoma.

Acknowledgments

Research supported by National Natural Science Funds of China (Grant #81202556) and Natural Science Foundation of Liaoning Province (Grant #20130222063).

References

- Jemal A, Bray F, Center MM, Ferlay J, Ward E, Forman D. Global cancer statistics. *CA Cancer J Clin* 2011; 61: 69-90, doi: 10.3322/caac.20107.
- Han KH, Park JY. Systemic treatment in advanced/metastatic hepatocellular carcinoma in the era of targeted therapy. *J Gastroenterol Hepatol* 2010; 25: 1023-1025, doi: 10.1111/j.1440-1746.2010.06359.x.
- Levin B, Amos C. Therapy of unresectable hepatocellular carcinoma. *N Engl J Med* 1995; 332: 1294-1296, doi: 10.1056/NEJM199505113321910.
- Hecht SS, Kenney PM, Wang M, Trushin N, Agarwal S, Rao AV, et al. Evaluation of butylated hydroxyanisole, myo-inositol, curcumin, esculetin, resveratrol and lycopene as inhibitors of benzo[a]pyrene plus 4-(methylnitrosamino)-1-(3-pyridyl)-1-butanone-induced lung tumorigenesis in A/J mice. *Cancer Lett* 1999; 137: 123-130, doi: 10.1016/S0304-3835(98)00326-7.
- Witaicenis A, Seito LN, Di Stasi LC. Intestinal anti-inflammatory activity of esculetin and 4-methylesculetin in the trinitrobenzenesulphonic acid model of rat colitis. *Chem Biol Interact* 2010; 186: 211-218, doi: 10.1016/j.cbi.2010.03.045.
- Yang J, Xiao YL, He XR, Qiu GF, Hu XM. Aesculetin-induced apoptosis through a ROS-mediated mitochondrial dysfunction pathway in human cervical cancer cells. *J Asian Nat Prod Res* 2010; 12: 185-193, doi: 10.1080/10286020903427336.
- Subramaniam SR, Ellis EM. Neuroprotective effects of umbelliferone and esculetin in a mouse model of Parkinson's disease. *J Neurosci Res* 2013; 91: 453-461, doi: 10.1002/jnr.23164.
- Pan SL, Huang YW, Guh JH, Chang YL, Peng CY, Teng CM. Esculetin inhibits Ras-mediated cell proliferation and attenuates vascular restenosis following angioplasty in rats. *Biochem Pharmacol* 2003; 65: 1897-1905, doi: 10.1016/S0006-2952(03)00161-8.
- Park SS, Park SK, Lim JH, Choi YH, Kim WJ, Moon SK. Esculetin inhibits cell proliferation through the Ras/ERK1/2 pathway in human colon cancer cells. *Oncol Rep* 2011; 25: 223-230.
- Park C, Jin CY, Kim GY, Choi IW, Kwon TK, Choi BT, et al. Induction of apoptosis by esculetin in human leukemia U937 cells through activation of JNK and ERK. *Toxicol Appl Pharmacol* 2008; 227: 219-228, doi: 10.1016/j.taap.2007.10.003.
- Kuo HC, Lee HJ, Hu CC, Shun HI, Tseng TH. Enhancement of esculetin on Taxol-induced apoptosis in human hepatoma HepG2 cells. *Toxicol Appl Pharmacol* 2006; 210: 55-62, doi: 10.1016/j.taap.2005.06.020.
- Jing Wang, Hong-yu Li, Hong-Xin Wang. The separation and purification technology of esculetin from CORTEX FRAXINI. *Chinese Traditional Patent Med* 2009; 31: 294-296.
- Wei N, Liu GT, Chen XG, Liu Q, Wang FP, Sun H. H1, a derivative of Tetrandrine, exerts anti-MDR activity by initiating intrinsic apoptosis pathway and inhibiting the activation of Erk1/2 and Akt1/2. *Biochem Pharmacol* 2011; 82: 1593-1603, doi: 10.1016/j.bcp.2011.08.012.
- Yokosuka T, Goto H, Fujii H, Naruto T, Takeuchi M, Tanoshima R, et al. Flow cytometric chemosensitivity assay using JC1, a sensor of mitochondrial transmembrane potential, in acute leukemia. *Cancer Chemother Pharmacol* 2013; 72: 1335-1342, doi: 10.1007/s00280-013-2303-x.
- Lavrik IN, Golks A, Krammer PH. Caspases: pharmacological manipulation of cell death. *J Clin Invest* 2005; 115: 2665-2672, doi: 10.1172/JCI26252.
- Jurgensmeier JM, Xie Z, Deveraux Q, Ellerby L, Bredesen D, Reed JC. Bax directly induces release of cytochrome c from isolated mitochondria. *Proc Natl Acad Sci U S A* 1998; 95: 4997-5002, doi: 10.1073/pnas.95.9.4997.
- Rubio V, Calvino E, Garcia-Perez A, Herraes A, Diez JC. Human acute promyelocytic leukemia NB4 cells are sensitive to esculetin through induction of an apoptotic mechanism. *Chem Biol Interact* 2014; 220C: 129-139, doi: 10.1016/j.cbi.2014.06.021.
- Holohan C, Van Schaeybroeck S, Longley DB, Johnston PG. Cancer drug resistance: an evolving paradigm. *Nat Rev Cancer* 2013; 13: 714-726, doi: 10.1038/nrc3599.
- Lee SY, Lim TG, Chen H, Jung SK, Lee HJ, Lee MH, et al. Esculetin suppresses proliferation of human colon cancer cells by directly targeting beta-catenin. *Cancer Prev Res* 2013; 6: 1356-1364, doi: 10.1158/1940-6207.CAPR-13-0241.
- Kok SH, Yeh CC, Chen ML, Kuo MY. Esculetin enhances TRAIL-induced apoptosis through DR5 upregulation in human oral cancer SAS cells. *Oral Oncol* 2009; 45: 1067-1072,

- doi: 10.1016/j.oraloncology.2009.07.018.
21. Lacy A, O'Kennedy R. Studies on coumarins and coumarin-related compounds to determine their therapeutic role in the treatment of cancer. *Curr Pharm Des* 2004; 10: 3797-3811, doi: 10.2174/1381612043382693.
 22. Hu W, Kavanagh JJ. Anticancer therapy targeting the apoptotic pathway. *Lancet Oncol* 2003; 4: 721-729, doi: 10.1016/S1470-2045(03)01277-4.
 23. Cullen SP, Martin SJ. Caspase activation pathways: some recent progress. *Cell Death Differ* 2009; 16: 935-938, doi: 10.1038/cdd.2009.59.
 24. Li J, Yuan J. Caspases in apoptosis and beyond. *Oncogene* 2008; 27: 6194-6206, doi: 10.1038/onc.2008.297.
 25. Kumar S. Caspase function in programmed cell death. *Cell Death Differ* 2007; 14: 32-43, doi: 10.1038/sj.cdd.4402060.
 26. Jiang X, Wang X. Cytochrome C-mediated apoptosis. *Annu Rev Biochem* 2004; 73: 87-106, doi: 10.1146/annurev-biochem.73.011303.073706.
 27. Czabotar PE, Lessene G, Strasser A, Adams JM. Control of apoptosis by the BCL-2 protein family: implications for physiology and therapy. *Nat Rev Mol Cell Biol* 2014; 15: 49-63, doi: 10.1038/nrm3722.
 28. Pastorino JG, Chen ST, Tafani M, Snyder JW, Farber JL. The overexpression of Bax produces cell death upon induction of the mitochondrial permeability transition. *J Biol Chem* 1998; 273: 7770-7775, doi: 10.1074/jbc.273.13.7770.
 29. Low IC, Kang J, Pervaiz S. Bcl-2: a prime regulator of mitochondrial redox metabolism in cancer cells. *Antioxid Redox Signal* 2011; 15: 2975-2987, doi: 10.1089/ars.2010.3851.
 30. Wong WW, Puthalakath H. Bcl-2 family proteins: the sentinels of the mitochondrial apoptosis pathway. *IUBMB Life* 2008; 60: 390-397, doi: 10.1002/iub.51.